JACC: BASIC TO TRANSLATIONAL SCIENCE
VOL. 1, NO. 6, 2016
ISSN 2452-302X
http://dx.doi.org/10.1016/j.jacbts.2016.07.008

PRECLINICAL RESEARCH

Atheroprotective Effects of Tumor Necrosis Factor–Stimulated Gene-6

Rena Watanabe, MS,[a] Hitomi Watanabe, MS,[a] Yui Takahashi, BS,[a] Miho Kojima, BS,[a] Hanae Konii, BS,[a] Kaho Watanabe, MS,[a] Remina Shirai, MS,[a] Kengo Sato, PhD,[a] Taka-aki Matsuyama, MD, PhD,[b] Hatsue Ishibashi-Ueda, MD, PhD,[b] Yoshitaka Iso, MD, PhD,[c] Shinji Koba, MD, PhD,[d] Youichi Kobayashi, MD, PhD,[d] Tsutomu Hirano, MD, PhD,[d] Takuya Watanabe, MD, PhD[a]

VISUAL ABSTRACT

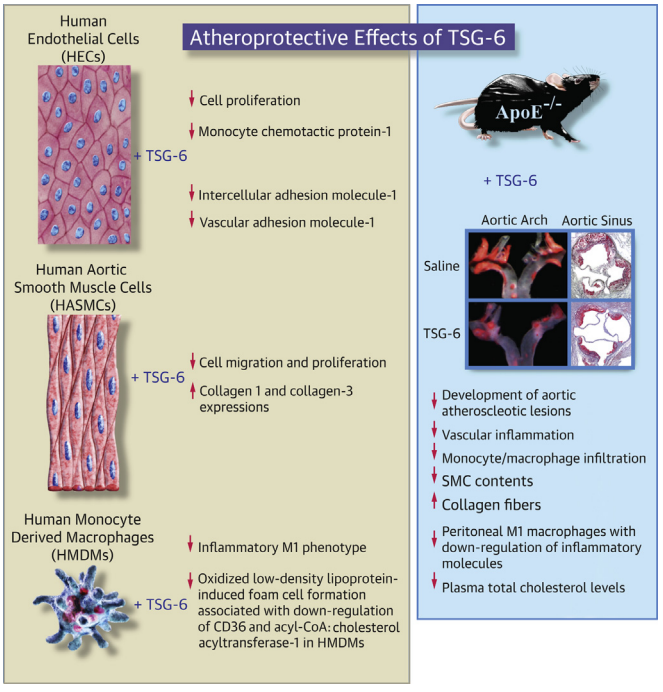

Watanabe, R. et al. J Am Coll Cardiol Basic Trans Science. 2016;1(6):494–509.

HIGHLIGHTS

- **TSG-6 suppresses the development of atherosclerosis by decreasing inflammatory responses of endothelial cells and macrophages, endothelial proliferation, macrophage foam cell formation, and VSMC migration and proliferation.**
- **TSG-6 also contributes to plaque stability by extracellular matrix production in the fibrous cap.**
- **TSG-6 is expected to emerge as a new line of therapy against atherosclerosis and CAD.**
- **This study also provides insights into the potential use of TSG-6 as a biomarker for CAD.**
- **These findings may strengthen the clinical utility of TSG-6 in the diagnosis and treatment of CAD.**

From the [a]Laboratory of Cardiovascular Medicine, Tokyo University of Pharmacy and Life Sciences, Tokyo, Japan; [b]Department of Pathology, National Cerebral and Cardiovascular Center, Osaka, Japan; [c]Showa University Research Institute for Sport and Exercise Sciences, Yokohama, Japan; and the [d]Department of Medicine, Showa University School of Medicine, Tokyo, Japan. This study was presented in part at the American Heart Association's Scientific Sessions 2014; Chicago, Illinois; November 15 to 19, 2014 (Circulation 2014;130:A9418). This work was supported in part by a Grant-in-Aid for Scientific Research (C) (26460659 to Dr. T. Watanabe) from the Japan Society for the Promotion of Science. The authors have reported that they have no relationships relevant to the contents of this paper to disclose.

Manuscript received June 30, 2016; revised manuscript received July 13, 2016, accepted July 25, 2016.

SUMMARY

Tumor necrosis factor–stimulated gene-6 (TSG-6), an anti-inflammatory protein, was shown to be localized in the neointima of injury-induced rat arteries. However, the modulatory effect of TSG-6 on atherogenesis has not yet been reported. We aimed to evaluate the atheroprotective effects of TSG-6 on human endothelial cells (HECs), human monocyte-derived macrophages (HMDMs), human aortic smooth muscle cells (HASMCs) in vitro, and aortic lesions in apolipoprotein E–deficient mice, along with expression levels of TSG-6 in coronary lesions and plasma from patients with coronary artery disease (CAD). TSG-6 was abundantly expressed in HECs, HMDMs, and HASMCs in vitro. TSG-6 significantly suppressed cell proliferation and lipopolysaccharide-induced up-regulation of monocyte chemotactic protein-1, intercellular adhesion molecule-1, and vascular adhesion molecule-1 in HECs. TSG-6 significantly suppressed inflammatory M1 phenotype and suppressed oxidized low-density lipoprotein–induced foam cell formation associated with down-regulation of CD36 and acyl-CoA:cholesterol acyltransferase-1 in HMDMs. In HASMCs, TSG-6 significantly suppressed migration and proliferation, but increased collagen-1 and -3 expressions. Four-week infusion of TSG-6 into apolipoprotein E–deficient mice significantly retarded the development of aortic atherosclerotic lesions with decreased vascular inflammation, monocyte/macrophage, and SMC contents and increased collagen fibers. In addition, it decreased peritoneal M1 macrophages with down-regulation of inflammatory molecules and lowered plasma total cholesterol levels. In patients with CAD, plasma TSG-6 levels were significantly increased, and TSG-6 was highly expressed in the fibrous cap within coronary atherosclerotic plaques. These results suggest that TSG-6 contributes to the prevention and stability of atherosclerotic plaques. Thus, TSG-6 may serve as a novel therapeutic target for CAD. (J Am Coll Cardiol Basic Trans Science 2016;1:494–509)

Tumor necrosis factor-stimulated gene (TSG)-6 is a 35-kDa secreted glycoprotein that has been shown to exert anti-inflammatory effects in experimental models of arthritis, acute myocardial infarction, and acute cerebral infarction (1–4). TSG-6 is not usually expressed but is rapidly up-regulated in many different cell types, including monocytes, fibroblasts, vascular smooth muscle cells (VSMCs), synoviocytes, chondrocytes, and proximal tubular epithelial cells by inflammatory mediators such as interleukin (IL)-1, tumor necrosis factor (TNF)-α, lipopolysaccharide (LPS), and prostaglandin E_2 (1,5–7). TSG-6 inhibits leukocyte adhesion onto the vascular wall and leukocyte migration (8,9). In addition, TSG-6 down-regulates toll-like receptor-2/nuclear factor (NF)-κB and up-regulates cyclooxygenase (COX)-2 in mouse macrophages (10,11). Although TSC-6 was shown to be localized in rat neointima after arterial injury and rabbit carotid atherosclerotic plaques (12,13), there have been no previous reports regarding its direct effect on atherogenesis.

Atherosclerosis is a chronic inflammatory response to arterial wall injuries (14). Endothelial inflammation stimulates the production of proinflammatory cytokines and molecules such as IL-6, monocyte chemotactic protein (MCP)-1, intercellular adhesion molecule (ICAM)-1, vascular adhesion molecule (VCAM)-1, and E-selectin in endothelial cells (ECs), and monocyte adhesion and infiltration into the neointima lesion (14). Macrophage foam cells participate in proinflammatory and anti-inflammatory responses via transition to M1 and M2 phenotypes by releasing and removing inflammatory mediators, such as TNF-α, IL-6, and oxidized low-density lipoprotein (oxLDL), within the arterial intima (15). Foam cell formation is characterized by the intracytoplasmic accumulation of cholesterol ester, which is dependent on the homeostatic balance between the uptake of oxLDL via CD36, the efflux of free cholesterol (FC) controlled by the ATP-binding cassette transporter A1 (ABCA1), and cholesterol esterification by acyl CoA:cholesterol acyltransferase-1 (ACAT1) (16,17). Apart from accumulation of macrophage foam cells, the migration and proliferation of VSMCs, EC proliferation, and the production of extracellular matrix (ECM) components such as collagen, matrix metalloproteinases (MMPs), tissue inhibitor of metalloproteinases (TIMPs), fibronectin, and elastin contribute to the progression of the atherosclerotic plaque (14,18).

In the present study, we assessed the suppressive effects of TSG-6 on the inflammatory responses in human ECs and human monocyte-derived macrophages (HMDMs); foam cell formation; the

ABBREVIATIONS AND ACRONYMS

ABCA1 = ATP-binding cassette transporter A1

ACAT1 = acyl-CoA:cholesterol acyltransferase-1

AngII = angiotensin II

ApoE$^{-/-}$ = apolipoprotein E deficient

CAD = coronary artery disease

ECM = extracellular matrix

HASMC = human aortic smooth muscle cell

HMDM = human monocyte-derived macrophage

HUVEC = human umbilical vein endothelial cell

MMP = matrix metalloproteinase

oxLDL = oxidized low-density lipoprotein

TIMP = tissue inhibitor of metalloproteinase

TSG = tumor necrosis factor stimulated gene

VSMC = vascular smooth muscle cell

migration, proliferation, and ECM production in human VSMCs in vitro; and the development of atherosclerotic lesions in an apolipoprotein E-deficient ($ApoE^{-/-}$) mouse model in vivo. Further, we investigated TSG-6 expression in coronary lesions and its plasma levels in patients with coronary artery disease (CAD).

METHODS

SAMPLE COLLECTION OF HUMAN BLOOD AND CORONARY ATHEROSCLEROTIC LESIONS. This study was conducted according to the principles of the Declaration of Helsinki and approved by the Ethics Committees of Showa University and Tokyo University of Pharmacy and Life Sciences. Written informed consent was obtained from a total of 182 participants before enrollment. Blood was collected from 135 patients with acute coronary syndrome hospitalized at Showa University Hospital for emergency coronary catheterization (102 men, 33 women; age 40 to 96 years) and 47 non-CAD subjects (32 men, 15 women; age 21 to 79 years). The patients with acute coronary syndrome included 103 patients with acute myocardial infarction and 32 patients with unstable angina pectoris. The non-CAD subjects included 23 healthy volunteers and 24 patients with mild hypertension, diabetes, or dyslipidemia. Infections and inflammatory diseases were excluded from subjects by history and routine laboratory examination because these are known to increase plasma TSG-6 levels (1,5). Plasma TSG-6 levels were measured by enzyme-linked immunosorbent assay (ELISA) (human TSG-6 ELISA kit, Cusabio Biotech, Wuhan, China).

Buffered 10% formalin-fixed paraffin-embedded human coronary artery specimens from archive collections of the National Cerebral and Cardiovascular Center were used for immunohistochemistry. The serial thin cross sections (3 to 4 μm) of stenotic and nonstenotic coronary arteries from 13 patients with a history of myocardial infarction (9 men, 4 women; age 60 to 87 years) and of normal coronary arteries from 4 patients with dilated cardiomyopathy (4 men; age 19 to 39 years) were stained with hematoxylin-eosin and Elastica van Gieson (19). Immunohistochemistry was performed on deparaffinized glass slides by the automated immunostainer BOND-III-TM (Leica Biosystems, Newcastle, United Kingdom). Polyclonal rabbit antibodies for human TSG-6 (LifeSpan BioSciences, Seattle, Washington) or von Willebrand factor and monoclonal mouse antibodies for human macrophage (CD68) or α-smooth muscle actin (α-SMA) (DAKO, Tokyo, Japan) were used as a primary antibody (19). The detection kit as a secondary antibody was the Bond Polymer Refine Detection (DS9800, Leica Biosystems); it involved incubation with post-primary for 8 min, polymer for 8 min, DAB for 10 min, and hematoxylin for 5 min. Masson's Trichrome staining for collagen fibers was also performed (19).

HUMAN MONOCYTE PRIMARY CULTURE. Human peripheral mononuclear cells were isolated from the blood of 20 healthy volunteers (10 men, 10 women; age 20 to 24 years). Monocytes purified using anti-CD14 antibody-conjugated magnetic microbeads (Miltenyi Biotec, Auburn, California) were seeded onto 3.5-cm dishes (1×10^6 cells per 1 ml/dish) for cholesterol esterification assay and immunoblotting analysis (19–23). Cells were incubated at 37°C in 5% CO_2 for 7 days with the indicated concentrations of human TSG-6 (R&D Systems, Minneapolis, Minnesota) in RPMI-1640 medium (Sigma, St. Louis, Missouri) supplemented with 10% human serum, 0.05 mg/ml streptomycin, and 50 U/ml penicillin. The medium in each dish was replaced with fresh medium containing TSG-6 every 3 days.

CHOLESTEROL ESTERIFICATION ASSAY. HMDMs differentiated by 10% human serum and the indicated concentrations of TSG-6 for 7 days were incubated for 19 h with the same concentrations of TSG-6 along with 50 μg/ml human oxLDL and 0.1 mmol/l [^{3}H] oleate (PerkinElmer, Yokohama, Japan) conjugated with bovine serum albumin (19,22,23). Cellular lipids were extracted, and the radioactivity of cholesterol-[^{3}H]oleate was determined by thin-layer chromatography.

ENZYME-LINKED IMMUNOSORBENT ASSAY. HMDMs differentiated by 10% human serum without TSG-6 were incubated for 26 h in serum-free RPMI-1640 medium with or without 300 ng/ml TSG-6. In culture supernatants, the concentrations of IL-6 and TNF-α were measured by ELISA (human IL-6 and human TNF-α ELISA kits, R&D Systems).

MIGRATION ASSAY. Human aortic smooth muscle cells (HASMCs) (Lonza, Walkersville, Maryland) at passage 7 or 8 were seeded onto an 8-well culture slide (3×10^3 cells per 200 μl/well). Cells were incubated at 37°C in 5% CO_2 for 3 to 5 h in smooth muscle cell basal medium (SmBM) supplemented with SmGM-2 SingleQuots (5% fetal bovine serum [FBS], 0.1% epidermal growth factor [EGF], 0.2% fibroblast growth factor [FGF], 0.1% insulin, and 0.1% gentamicin-amphotericin B mixture) and were then incubated for 24 h in serum-free SmBM. Subsequently, while cells were incubated for 15 h in serum-free SmBM with 500 nmol/l angiotensin II (AngII) (Sigma) and/or 300 ng/ml TSG-6, photographs of cells were taken for the last 5 h at 10-min intervals. The average migration

distance of 10 cells randomly selected in each well was measured using a BIOREVO BZ-9000 microscope (Keyence, Osaka, Japan) (19,22,23).

PROLIFERATION ASSAY. HASMCs or human EA.hy926 ECs at passage 8 or 9 were seeded onto 96-well plates (1×10^4 cells per 100 μl/well) and incubated at 37°C in 5% CO_2 for 24 h in SmBM supplemented with SmGM-2 SingleQuots (Lonza) or in Dulbecco's Modified Eagle's Medium (Sigma) supplemented with 10% FBS, 1.0 mg/ml D-glucose/4.5 mg/ml D-glucose, 0.584 mg/ml L-glutamine, 0.05 mg/ml streptomycin, and 50 U/ml penicillin. Cells were incubated for 48 h with the indicated concentrations of TSG-6 with renewal of each medium. Then, 10 μl of WST-8 solution (Cell Count Reagent SF, Nacalai Tesque, Kyoto, Japan) were added to each well (19,22,23). After 1 h of incubation, the amount of formazan product was determined by measuring the absorbance at 450 nm using a Sunrise Remote R-microplate reader (Tecan, Kawasaki, Japan) (19,22,23).

WESTERN BLOTTING. Aliquots of 20 μg of protein extracts from HMDMs and HASMCs were separated by 10% sodium dodecyl sulfate-polyacrylamide gel electrophoresis and subjected to immunoblotting with antibodies for TSG-6 (ProteinTech Group, Chicago, Illinois), CD36 (R&D Systems), CD68, ACAT1 (Santa Cruz Biotechnology, Santa Cruz, California), ABCA1, collagen-1 (Novus Biologicals, Littleton, Colorado), collagen-3, fibronectin, JNK, α-tubulin, MMP-2 (GeneTex, Irvine, California), MMP-9 (Eno-Gene, Atlanta, Georgia), TIMP-2 (Abbiotec, San Diego, California), elastin, MARCO (Bioss, Woburn, Massachusetts), MRC1 (LifeSpan BioSciences, Seattle, Washington), phosphoinositide 3-kinase (PI3K), Raf-1 (Abcam, Tokyo, Japan), c-Src (Bioworld Technology, St. Louis Park, Minnesota), phosphorylated ERK1/2 (Cell Signaling Technology, Tokyo, Japan), NF-κB (Aviva Systems Biology, San Diego, California), or β-actin (Sigma) (19–23).

ZYMOGRAPHY. The activities of MMP-2 and -9 were determined using a gelatin zymography kit (Cosmo Bio, Tokyo, Japan) (23). The culture supernatants of HASMCs (15 μg) were mixed with 5 μl of sample buffer and fractionated by 10% sodium dodecyl sulfate-polyacrylamide gel electrophoresis using 0.1% gelatin. After electrophoresis, the gel was washed with renaturing buffer (2% Triton X-100) for 1 h. The gel was incubated for 20 h at 37°C in a reaction buffer (1% Triton X-100) and then was stained with Coomassie brilliant blue (23).

REVERSE TRANSCRIPTION-POLYMERASE CHAIN REACTION. Human umbilical vein endothelial cells (HUVECs) (Lonza) at passage 4 to 7 were seeded onto 3.5-cm dishes and incubated at 37°C in 5% CO_2 for 24 h in endothelial growth basal medium (EBM)-2 supplemented with EGM-2 SingleQuots + FBS (5% FBS, 0.1% EGF, 0.4% FGF, 0.1% VEGF, 0.1% heparin, 0.04% hydrocortisone, 0.1% R3-IGF-1, and 0.1% gentamicin-amphotericin B mixture). When cells reached 60% to 70% confluence, they were incubated for 30 min with 300 ng/ml TSG-6 and then for 2 h with 1 μg/ml LPS (Sigma) and/or 300 ng/ml TSG-6 (23). Total ribonucleic acid (RNA) was extracted using a High Pure RNA Isolation Kit (Roche Diagnostics, Mannheim, Germany). Complementary DNA was synthesized from isolated RNA templates with a High Capacity cDNA Reverse Transcription Kit (Applied Biosystems, Foster City, California). The messenger ribonucleic acid (mRNA) of IL-6, TNF-α, MCP-1, ICAM-1, VCAM-1, E-selectin, and glyceraldehyde-3-dehydrogenase in 50 ng of each sample were detected by reverse transcription-polymerase chain reaction, using GoTaq Green Master Mix (Promega, Madison, Wisconsin) (23–25). The sequences of the primers and product sizes are listed in **Table 1**. The polymerase chain reaction products were separated by 2% agarose gel electrophoresis.

TABLE 1 Primer Sequences Used for Reverse Transcription Polymerase Chain Reaction

Gene		Primer Sequence (5′→3′)	Product Size (bp)
IL-6	Forward	ATGAACTCCTTCTCCACAAGCGC	628
	Reverse	GAAGAGCCCTCAGGCTGGACT	
TNF-α	Forward	CAGAGGGAAGAGTTCCCCAG	325
	Reverse	CCTTGGTCTGGTAGGAGACG	
MCP-1	Forward	CAATAGGAAGATCTCAGTGC	189
	Reverse	GTGTTCAAGTCTTCGGAGTT	
ICAM-1	Forward	CGACTGGACGACAGGGATTGT	290
	Reverse	ATTATGACTGCGGCTGCTACC	
VCAM-1	Forward	TCCCTACCATTGAAGATACTGGAAA	146
	Reverse	GCTGACCAAGACGGTTGTATCTC	
E-selectin	Forward	CCTACAAGTCCTCTTGTGCCTTC	206
	Reverse	ACAGGCGAACTTGCACACA	
GAPDH	Forward	ACCACAGTCCATGCCATCAC	451
	Reverse	TCCACCACCCTGTTGCTGTA	

GAPDH = glyceraldehyde-3-dehydrogenase; IL = interleukin; MCP = monocyte chemotactic protein; ICAM = intercellular adhesion molecule; TNF = tumor necrosis factor; VCAM = vascular adhesion molecule.

ANIMAL EXPERIMENTS. Animal experiments were performed in accordance with the National Institutes of Health Guidelines for the Care and Use of Laboratory Animals and approved by the Institutional Animal Care and Use Committee of Tokyo University of Pharmacy and Life Sciences. A total of 28 male, spontaneously hyperlipidemic, 9-week-old ApoE$^{-/-}$ mice (C57BL/6. KOR/StmSlc-*Apoe*^{shl} mice) were

purchased from Japan SLC Inc. (Hamamatsu, Japan) and maintained on a normal diet until they reached the age of 13 weeks. Then, a high-cholesterol diet (Oriental Yeast, Tokyo, Japan) was started (19,22,23). Two groups of 17-week-old ApoE$^{-/-}$ mice were infused with saline (vehicle) or TSG-6 (75 ng/kg/min) (GenWay Biotech, San Diego, California) for 4 weeks using osmotic mini-pumps (Alzet Model 1002, Durect, Cupertino, California) (19,22). The doses of TSG-6 were decided on the basis of our preliminary examinations and a previous report (26).

Systolic and diastolic blood pressures were measured using the indirect tail-cuff method (Kent Scientific, Torrington, Connecticut). Four days before the endpoint of infusion, mice were intraperitoneally injected with 2 ml of aged-autoclaved thioglycolate broth to obtain exudate peritoneal macrophages, which is thought to mimic arterial macrophages present in atheroma areas (22,27). Exudate peritoneal macrophages are widely accepted to use in the assessment of mouse atherosclerosis (22,27).

At the experimental endpoint (before and 4 weeks after infusion), the ApoE$^{-/-}$ mice were sacrificed by exsanguination (total blood collection) under deep ether anesthesia (19,21–23). Peritoneal cells were sampled by needle aspiration (19,21–23). The whole aorta was immediately washed by perfusion with PBS and was fixed with 4% formaldehyde (19,21–23). The aorta was excised from the aortic root to the abdominal area, and the connective and adipose tissues were carefully removed.

ATHEROSCLEROTIC LESION ASSESSMENT. The entire aorta lumen surface and cross sections of the aortic sinus were stained with oil red O for assessment of atherosclerotic lesion area and plaque size, respectively (19,21–23). In aortic sinus, vascular inflammation, intra-plaque monocyte/macrophage and VSMC contents, and collagen fibers were visualized by staining with antibodies for pentraxin-3 (Bioss), MOMA-2 (Millipore, Billerica, Massachusetts), or α-SMA (Sigma) and Masson's Trichrome (Muto Pure Chemicals, Tokyo, Japan), respectively (19,22,23). The positive stained areas were traced by an investigator blind to the treatment and measured using image analysis software (Adobe Photoshop, San Jose, California; and NIH ImageJ, Bethesda, Maryland). The degree of vascular inflammation derived from mainly ECs followed by VSMCs and macrophages was expressed as a percentage of the pentraxin-3-positive area relative to the entire cross section of the aortic wall (21,27).

MOUSE PERITONEAL EXUDATE MACROPHAGE ASSESSMENT. Peritoneal cells were immediately suspended in RPMI-1640 medium supplemented with 10% FBS, 0.05 mg/ml streptomycin, and 50 U/ml penicillin, and were seeded onto 6-cm dishes (4×10^6 cells per 2 ml/dish). After incubation for 1 h at 37°C in 5% CO_2 to allow adhesion, the medium was discarded to remove nonadherent cells. Adherent macrophages were immediately harvested after washing the dishes with PBS twice for immunoblotting with antibodies to pentraxin-3, MARCO (Bioss), arginase-1, MCP-1, JNK (GeneTex), COX-2 (Cayman Chemical, Ann Arbor, Michigan), NF-κB (Aviva Systems Biology), phosphorylated ERK1/2 (Cell Signaling Technology), or β-actin (Sigma) (19,22).

BLOOD SAMPLE MEASUREMENTS. Fasting plasma glucose and total cholesterol levels were measured by enzymatic methods (Denka Seiken, Tokyo, Japan) and high-density lipoprotein (HDL) levels were measured by a precipitation method (Wako, Osaka, Japan) (19,21–23). Plasma levels of TSG-6 and pentraxin-3 were measured by ELISA (Cusabio Biotech, R&D Systems).

STATISTICAL ANALYSIS. Results are expressed as mean ± SEM for continuous variables and as percentages for categorical variables. Normal distribution of continuous variables was assessed using the Kolmogorov-Smirnov test. On the basis of the normality of the variables, the parametric or the nonparametric test was chosen as appropriate. Comparisons between 2 groups were made using the unpaired Student *t* test or the Mann-Whitney *U* test. Multiple comparisons were made among ≥3 groups using 1-way analysis of variance or the Kruskal-Wallis test followed by the Bonferroni post-hoc test. The categorical variables were analyzed using the chi-square test. Multiple linear regression analysis was performed to evaluate the predictor variables for plasma TSG-6 levels. Pearson's correlation coefficient was used to evaluate the linear relationship between plasma TSG-6 levels and other variables. Statistical analyses were performed using Statview-J version 5.0 (SAS Institute, Cary, North Carolina) and SPSS version 22.0 (SPSS Inc., Chicago, Illinois). A value of $p < 0.05$ was considered to indicate statistical significance.

RESULTS

EXPRESSION OF TSG-6 IN HUMAN VASCULAR CELLS IN VITRO. TSG-6 was expressed at infinitesimal levels in human monocytes but at high levels in HMDMs, HASMCs, and HUVECs (**Figure 1A**). The independent experiment that was repeated once more also confirmed the same results. The results were consistent with the previous reports (1,5–7).

FIGURE 1 Expression of TSG-6 in Human Vascular Cells and its Effects on Inflammatory Response and Proliferation in Human ECs

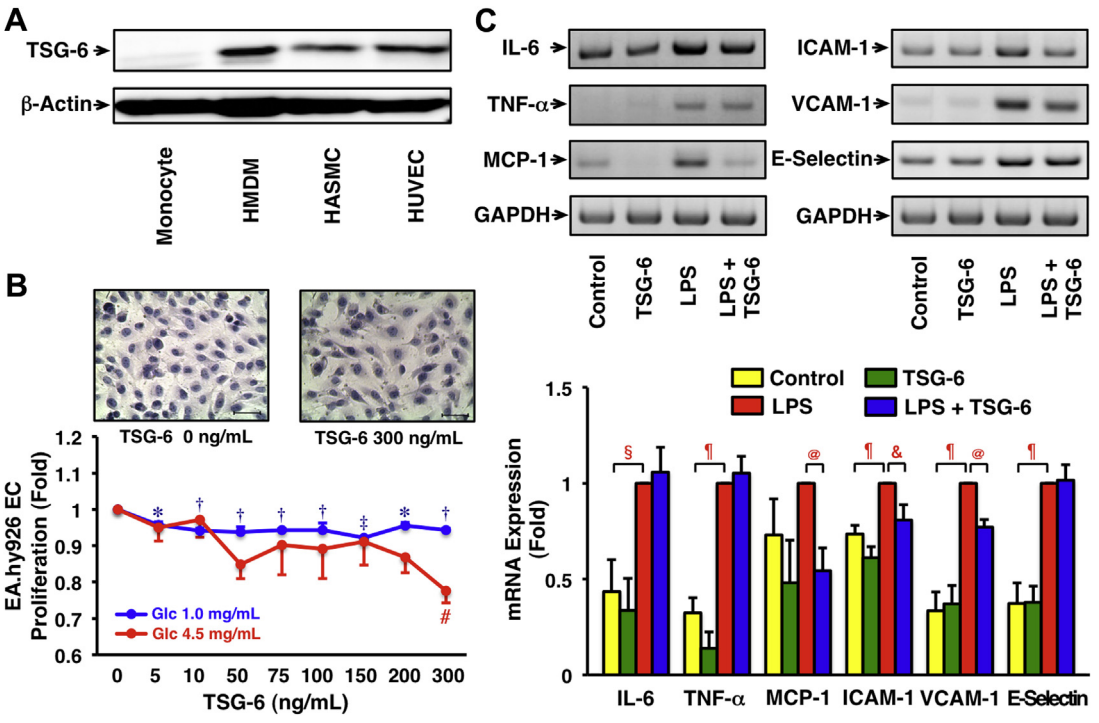

(A) Aliquots of 40 μg of cellular protein from human monocytes, HMDMs, HASMCs, and HUVECs were separated by 10% sodium dodecyl sulfate-polyacrylamide gel electrophoresis and subjected to immunoblotting analysis for human TSG-6 and β-actin. Immunoblots are representative of 2 independent experiments. **(B)** Proliferation of EA.hy926 ECs was determined by WST-8 assay after 48-h incubation in DMEM containing 2 concentrations of D-glucose (Glc) (1.0 or 4.5 mg/ml) with the indicated concentrations of TSG-6. EA.hy926 ECs cultured in 4.5 mg/ml D-glucose–conditioned medium were stained by hematoxylin eosin. Glc 1.0 mg/ml **(blue)**: n = 4; *p < 0.005; †p < 0.0005; ‡p < 0.0001 vs. 0 ng/ml of TSG-6. Glc 4.5 mg/ml **(red)**: n = 5; #p < 0.01 vs. 0 ng/ml of TSG-6. **(C)** HUVECs were pre-treated with or without TSG-6 (300 ng/ml) for 30 min and then incubated with or without LPS (1 μg/ml) for 2 h. The levels of IL-6, TNF-α, MCP-1, ICAM-1, VCAM-1, E-selectin, and GADPH mRNA expression were measured by reverse transcription polymerase chain reaction. The **graph** shows the densitometric data of each molecule after normalization relative to GADPH. n = 3 to 4; §p = 0.028; ¶p < 0.005 vs. control; @p < 0.01; &p = 0.028 vs. LPS. All values are presented as mean ± SEM. EC = endothelial cells; GAPDH = glyceraldehyde-3-dehydrogenase; Glc = D-glucose; HASMC = human aortic smooth muscle cell; HMDM = human monocyte-derived macrophage; HUVEC = human umbilical vein endothelial cell; ICAM = intercellular adhesion molecule; IL = interleukin; LPS = lipopolysaccharide; MCP = monocyte chemotactic protein; mRNA = messenger ribonucleic acid; TNF = tumor necrosis factor; TSG = tumor necrosis factor–stimulated gene; VCAM = vascular adhesion molecule.

EFFECTS OF TSG-6 ON PROLIFERATION AND INFLAMMATORY RESPONSE IN HUMAN ECs. In a normal glucose condition (1.0 mg/ml), TSG-6 at 5 to 300 ng/ml significantly suppressed the proliferation of EA.hy926 ECs, with the maximal reduction by ~10% (Figure 1B). In a high glucose condition (4.5 mg/ml), TSG-6 significantly suppressed the proliferation only at 300 ng/ml, with a maximal reduction of ~25% (Figure 1B). The micrographs confirmed that the reduction in cell number was not attributed to death due to apoptosis and cytotoxicity by 4.5 mg/ml glucose and/or 300 ng/ml TSG-6 (Figure 1B). These observations suggest that the antiproliferative effects of TSG-6 may be accentuated under the condition of hyperglycemia-induced endothelial dysfunction.

TSG-6 itself had no significant effects on mRNA expressions of IL-6, TNF-α, MCP-1, ICAM-1, VCAM-1, and E-selectin, but LPS markedly stimulated these expressions in HUVECs (Figure 1C). However, TSG-6 at 300 ng/ml significantly suppressed LPS-induced mRNA expressions of MCP-1, ICAM-1, and VCAM-1, but not IL-6, TNF-α, and E-selectin, in HUVECs (Figure 1C).

EFFECTS OF TSG-6 ON INFLAMMATORY PHENOTYPE AND CYTOKINE SECRETION IN HMDMs. After 3 to 6 days of primary culture, the differentiation of human monocytes into HMDMs was confirmed by the increased protein expression of CD68, a macrophage differentiation marker (Figure 2A). TSG-6 did not affect

FIGURE 2 Effects of TSG-6 on Inflammatory Phenotypes, Cytokine Secretion, Foam Cell Formation, and Related Protein Expression in HMDMs

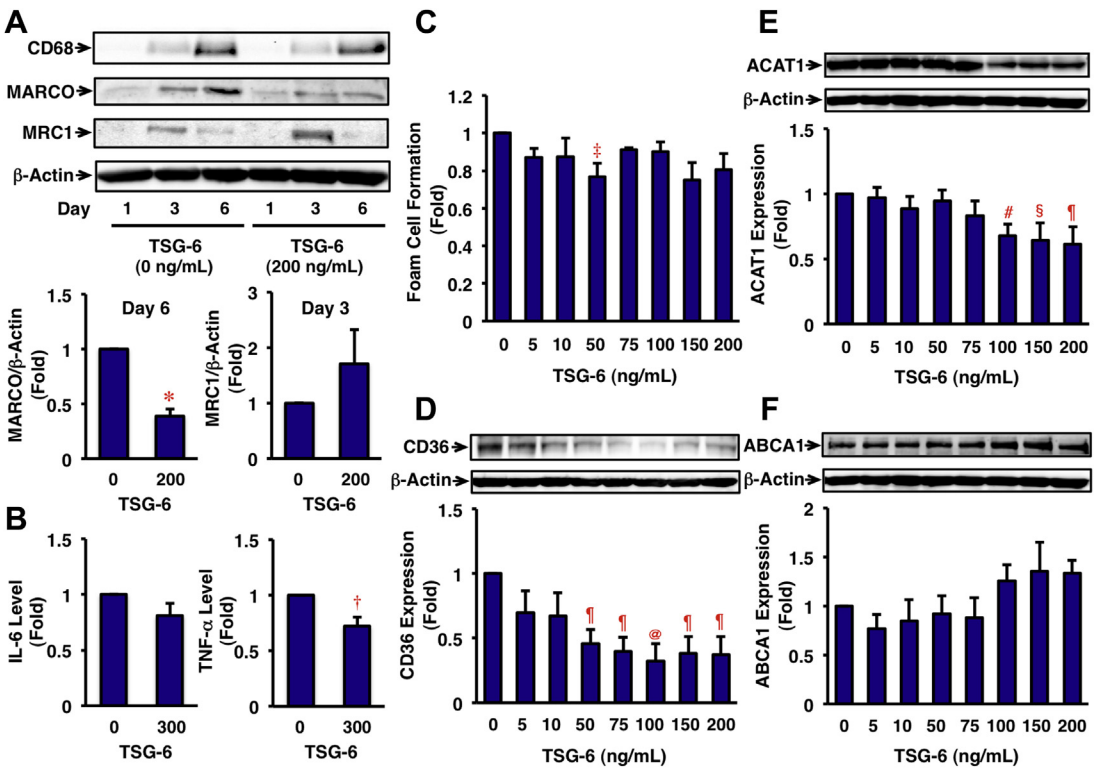

(A) Human monocytes were incubated for the indicated times in RPMI-1640 medium containing 10% human serum with or without TSG-6 (200 ng/ml). Cells were harvested for immunoblotting analysis for CD68 (differentiation marker), MARCO (M1 marker), or MRC1 (M2 marker). β-actin served as a loading control. The **graph** shows the expressions of MARCO on day 6 and MRC1 on day 3. n = 3; *p < 0.001 vs. 0 ng/ml of TSG-6. **(B)** HMDMs differentiated by 10% human serum without TSG-6 were incubated for 26 h in serum-free RPMI-1640 medium with or without TSG-6 (300 ng/ml). The concentrations of IL-6 and TNF-α in culture supernatants were measured by enzyme-linked immunosorbent assay. Baseline of control = 27.3 ± 11.9 pg/ml (IL-6) and 34.7 ± 3.1 pg/ml (TNF-α). n = 3; †p = 0.028 vs. control. **(C)** Human monocytes were incubated to differentiate into HMDMs for 7 days in RPMI-1640 with 10% human serum and the indicated concentrations of TSG-6, followed by a further 19 h with the same concentrations of TSG-6, 50 μg/ml oxLDL, and 0.1 mmol/l [^{3}H]oleate. Foam cell formation was determined from the intracellular radioactivity of cholesterol-[^{3}H]oleate. Baseline of control = 11.8 ± 4.0 nmol/mg cell protein. n = 4; ‡p = 0.042 vs. 0 ng/ml of TSG-6. **(D to F)** Before the addition of oxLDL, HMDMs were harvested for immunoblotting analysis of CD36, ACAT1, or ABCA1. β-actin served as a loading control. n = 6 to 7; #p = 0.021; §p = 0.014; ¶p < 0.01; and @p < 0.001 vs. 0 ng/ml of TSG-6. All values are presented as mean ± SEM. ACAT1 = acyl-CoA:cholesterol acyltransferase-1; oxLDL = oxidized low-density lipoprotein; other abbreviations as in Figure 1.

monocyte differentiation into HMDMs. However, TSG-6 significantly decreased the expression of MARCO, an M1 marker, on day 6 and showed a tendency to increase the expression of MRC1, an M2 marker, only on day 3 but not on day 6. These observations indicated that TSG-6 shifted the macrophage phenotype overwhelmingly to M2 rather than M1.

As shown in Figure 2B, TSG-6 showed a tendency to suppress IL-6 secretion and significantly suppressed TNF-α secretion from HMDMs. However, TSG-6 did not significantly suppress the LPS-induced IL-6 and TNF-α secretion from HMDMs (Supplemental Figure 1).

EFFECTS OF TSG-6 ON FOAM CELL FORMATION IN HMDMs. TSG-6 significantly suppressed oxLDL-induced foam cell formation by 25% at 50 ng/ml in HMDMs (Figure 2C). In HMDMs just before oxLDL was added, TSG-6 significantly suppressed CD36 and ACAT1 protein expression (Figures 2D and 2E) and showed a tendency to increase ABCA1 protein expression (Figure 2F) in a concentration-dependent manner.

EFFECTS OF TSG-6 ON MIGRATION AND PROLIFERATION IN HUMAN VSMCs. TSG-6 significantly suppressed the proliferation of HASMCs in a concentration-dependent manner, with the maximal reduction by

FIGURE 3 Effects of TSG-6 on Proliferation, Migration, and Signal Transduction in Human VSMCs

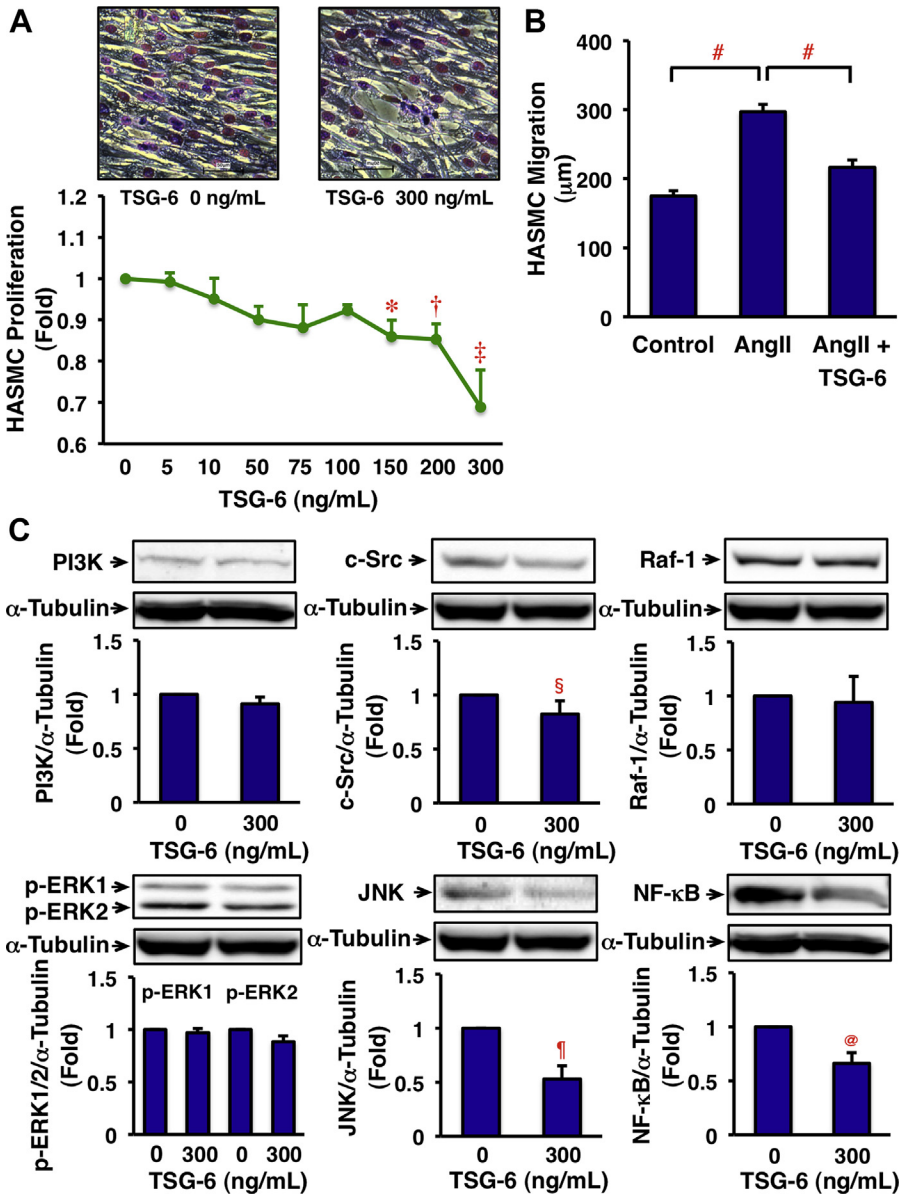

(A) Proliferation of HASMCs was determined by WST-8 assay after 48-h incubation in conditioned medium with the indicated concentrations of TSG-6. HASMCs were stained with Giemsa. n = 5; *p = 0.035; †p = 0.029; ‡p < 0.0001 vs. 0 ng/ml of TSG-6. **(B)** Migration of HASMCs was determined in 10 cells/well using a BIOREVO BZ-9000 microscope in serum-free medium with or without AngII (500 nmol/l) and/or TSG-6 (300 ng/ml). n = 30 from 3 independent experiments. #p < 0.0001. **(C)** To assess their signal transductions, HASMCs that were incubated for 48 h with or without TSG-6 (300 ng/ml) were subjected to immunoblotting analysis for PI3K, c-Src, Raf-1, phosphorylated ERK1/2, JNK, and NF-κB. α-tubulin served as a loading control. n = 3 to 4; §p = 0.035; ¶p = 0.020; @p = 0.013 vs. 0 ng/ml of TSG-6. All values are presented as mean ± SEM. AngII = angiotensin II; NF-κB = nuclear factor-κB; p-ERK = phosphorylated ERK; PI3K = phosphoinositide 3-kinase; VSMC = vascular smooth muscle cell; other abbreviations as in Figure 1.

31% at 300 ng/ml (Figure 3A). The reduction in cell number was not attributed to death due to apoptosis and cytotoxicity by 300 ng/ml TSG-6 (Figure 3A). In addition, the migration of HASMCs was significantly increased by the treatment with 500 nmol/l AngII (Figure 3B). However, TSG-6 significantly suppressed the AngII-induced migration of HASMCs (Figure 3B).

TSG-6 significantly suppressed the protein expression of c-Src, JNK, and NF-κB, but not PI3K, Raf-1, and phosphorylated ERK1/2 in HASMCs (Figure 3C). As exhibited in Supplemental Figure 2A, TSG-6 increased the protein expression of Bcl-2, an antiapoptotic molecule, and decreased that of p38, a proapoptotic molecule, without affecting both contractile and synthetic phenotypes (α-SMA and SMemb) in HASMCs.

EFFECTS OF TSG-6 ON ECM EXPRESSION AND ACTIVITY IN HUMAN VSMCs. TSG-6 significantly increased the protein expression of collagen-1, collagen-3, MMP-2, and TIMP-2 and showed a tendency to increase MMP-9, fibronectin, and elastin in HASMCs (Figure 4A). Further, TSG-6 significantly increased the activities of MMP-2 and -9 in a concentration-dependent manner (Figure 4B).

EFFECTS OF TSG-6 ON ATHEROSCLEROTIC LESION DEVELOPMENT IN ApoE$^{-/-}$ MICE. In 21-week-old compared with 17-week-old ApoE$^{-/-}$ mice, aortic atherosclerotic lesions in both the entire surface area and the cross-sectional area of the sinus (plaque size) significantly developed by 2-fold (Figures 5A, 5B, 5D, 5E, 5S, and 5T), whereas body weight significantly increased by 15% (Table 2). At 21 weeks of age, TSG-6 levels in plasma were significantly increased by 1.6-fold in TSG-6-infused mice compared with their saline-infused counterparts (Table 2). Chronic

FIGURE 4 Effects of TSG-6 on ECM Expression in Human VSMCs

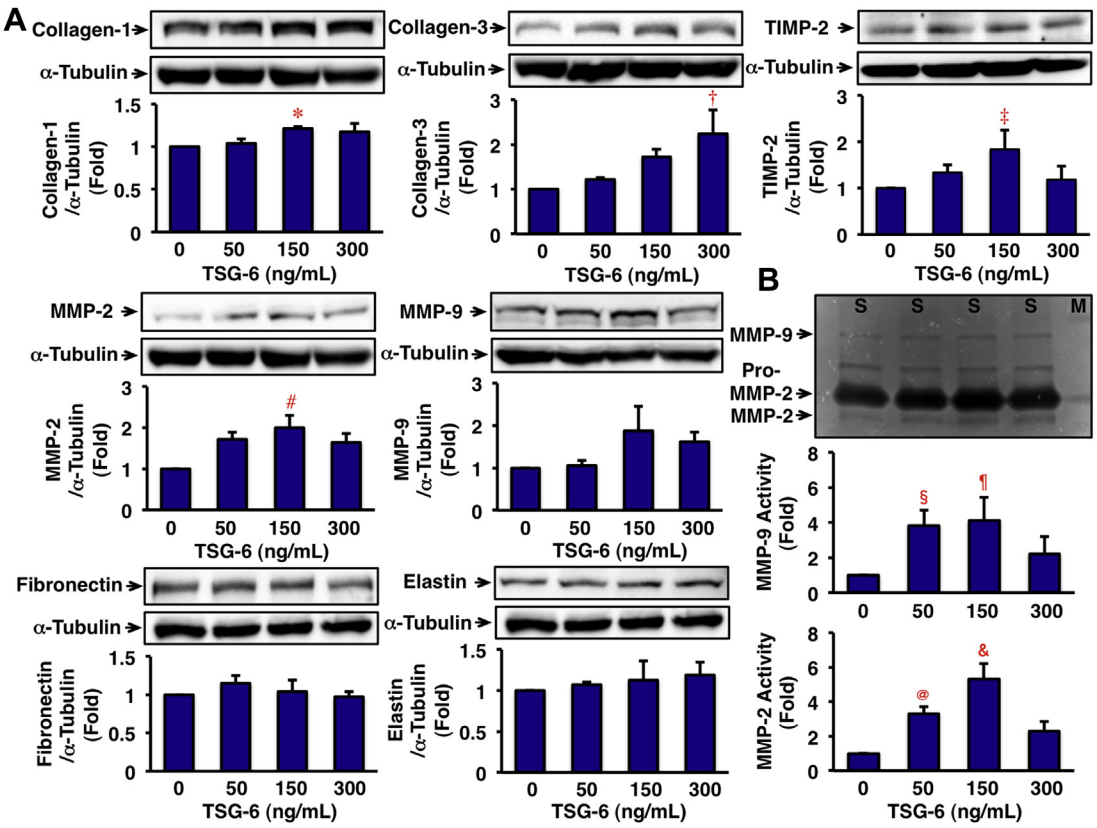

(A) HASMCs were incubated for 24 h with the indicated concentrations of TSG-6 and were harvested for immunoblotting analyses of collagen-1, collagen-3, TIMP-2, MMP-2, MMP-9, fibronectin, elastin, and α-tubulin. **(Top)** Representative results of protein expression of each molecule. **(Bottom)** Densitometric data of each molecule after normalization relative to α-tubulin. n = 4 to 7; *p = 0.025; †p = 0.015; ‡p = 0.047; #p < 0.01 vs. 0 ng/ml of TSG-6. **(B)** HASMCs were incubated for 24 h in serum-free conditioned medium with the indicated concentrations of TSG-6. In the culture supernatant, MMP-2 and -9 activities were determined by the gelatin zymography. n = 5 to 6; §p = 0.049; ¶p = 0.031; @p = 0.011; &p < 0.0001 vs. 0 ng/ml of TSG-6. All values are presented as mean ± SEM. ECM = extracellular matrix; M = matrix metalloproteinase marker; MMP = matrix metalloproteinase; S = sample; TIMP = tissue inhibitor of metalloproteinase; VSMC = vascular smooth muscle cell; other abbreviations as in Figure 1.

FIGURE 5 **Effects of TSG-6 on Atherosclerotic Lesion Development in ApoE$^{-/-}$ Mice**

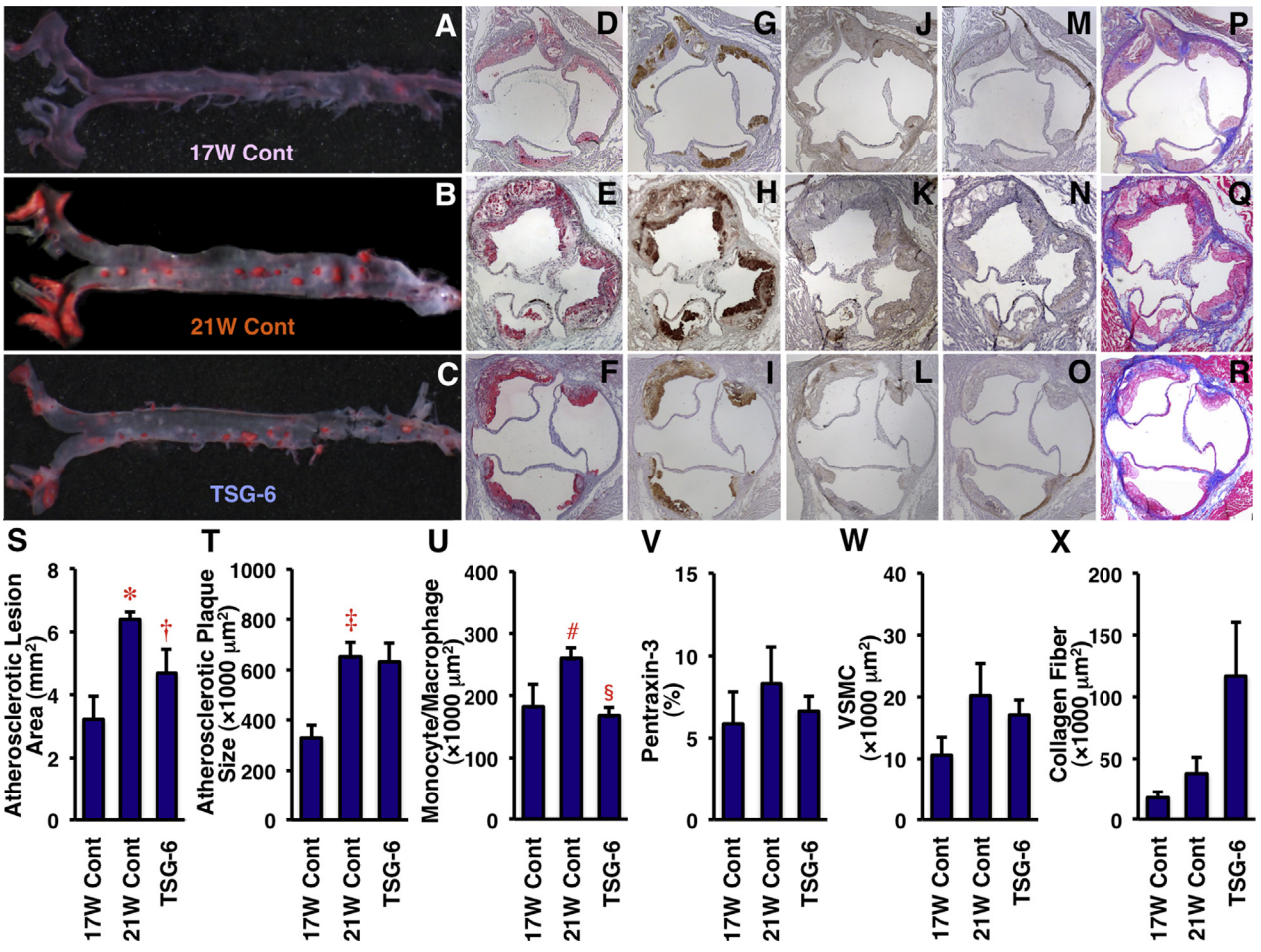

Among 28 ApoE$^{-/-}$ mice at 17 weeks of age, 6 mice were sacrificed before infusion, and 13 and 9 mice were infused with saline (control) or TSG-6 (75 ng/kg/min), respectively, by osmotic minipumps for 4 weeks. The aortic surface was stained by oil red O **(A to C)**. Cross sections of the aortic sinus were stained with oil red O **(D to F)**; antibodies of MOMA-2, a monocyte-macrophage marker **(G to I)**; pentraxin-3, a vascular inflammation marker **(J to L)**; α-SMA, a VSMC marker **(M to O)**; and Masson's trichrome, a collagen fiber marker **(P to R)**. Hematoxylin was used for nuclear staining. **(S to X)** Comparisons of atherosclerotic lesion area, plaque size, intraplaque monocyte/macrophage and VSMC contents, vascular inflammation, and collagen fibers among the 3 groups. *$p < 0.001$; ‡$p < 0.01$; #$p = 0.022$ vs. 17-week control; †$p = 0.024$; §$p < 0.005$ vs. 21-week control. All values are presented as mean ± SEM. ApoE$^{-/-}$ = apolipoprotein E deficient; Cont = control; SMA = smooth muscle actin; TSG = tumor necrosis factor–stimulated gene; VSMC = vascular smooth muscle cell.

infusion of TSG-6 significantly retarded the surface areas of the atherosclerotic lesions by 30% (Figures 5B, 5C, and 5S), with little reduction of plaque size in the sinus (Figures 5E, 5F, and 5T). In the atherosclerotic plaque, there was a significant reduction of monocyte/macrophage infiltration (Figures 5H, 5I, and 5U). TSG-6 was prone to decreasing vascular inflammation (Figures 5K, 5L, and 5V) and VSMC contents (Figures 5N, 5O, and 5W) along with increasing collagen fibers (Figures 5Q, 5R, and 5X).

Chronic infusion of TSG-6 significantly decreased cell number (Table 2), and protein expression of MARCO (M1 marker), MCP-1, COX-2, NF-κB, and phosphorylated ERK1/2, but not arginase-1 (M2 marker) in peritoneal exudate macrophages (Figure 6). TSG-6 also showed a tendency to decrease pentraxin-3 and JNK expression (Figure 6). As exhibited in Supplemental Figure 2B, TSG-6 suppressed other inflammatory molecules such as C-reactive protein (CRP), apoptosis-associated speck-like protein containing a caspase recruitment domain, and TNF-α–induced protein-1.

There were no significant differences in body weight, systolic and diastolic blood pressures, or plasma levels of glucose and pentraxin-3 between the 2 groups of ApoE$^{-/-}$ mice at 21 weeks of age (Table 2).

TABLE 2 Characteristics and Laboratory Data of ApoE$^{-/-}$ Mice

	17-Week Controls (n = 6)	21-Week Controls (n = 13)	TSG-6 (n = 9)
Body weight, g	26.7 ± 0.7	30.5 ± 0.4*	31.0 ± 0.7*
Systolic blood pressure, mm Hg	106.2 ± 5.6	94.0 ± 2.3	106.6 ± 3.7
Diastolic blood pressure, mm Hg	84.2 ± 6.1	74.9 ± 2.6	76.8 ± 5.4
TSG-6, ng/ml	0.97 ± 0.16	1.00 ± 0.10	1.59 ± 0.26†
Glucose, mg/dl	173.3 ± 13.1	206.3 ± 25.0	186.8 ± 10.0
Total cholesterol, mg/dl	1,639.5 ± 68.5	1,766.3 ± 64.8	1,572.2 ± 52.8‡
HDL cholesterol, mg/dl	6.68 ± 1.50	6.55 ± 1.05	8.48 ± 1.31
Pentraxin-3, ng/ml	111.8 ± 26.9	108.6 ± 6.7	116.8 ± 9.8
Peritoneal exudate cells, × 10^7	NE	0.56 ± 0.02	0.23 ± 0.06§

Values are mean ± SEM. *p < 0.005 vs. 17-week controls; †p = 0.033; ‡p = 0.043; §p < 0.005 vs. 21-week controls.

ApoE$^{-/-}$ = apolipoprotein E deficient; HDL = high-density lipoprotein; NE = not examined; TSG = tumor necrosis factor–stimulated gene.

However, TSG-6 significantly decreased plasma total cholesterol levels and showed a tendency to increase HDL cholesterol levels.

PRESENCE OF TSG-6 IN HUMAN CORONARY ARTERY LESIONS AND PLASMA. The levels of TSG-6 expression were assessed in human coronary arteries from 4 patients without CAD and 13 with CAD. Expression of TSG-6 was minimal in normal and nonstenotic coronary arteries from a patient without CAD and a patient with CAD, respectively (Figures 7A to 7D). In the stenotic coronary artery from another patient with CAD, TSG-6 was highly expressed in the fibrous cap within atherosclerotic plaques (Figures 7E and 7F), which were indicated by consistent areas stained blue with Masson's Trichrome (Figure 7H). The remaining patients with and without CAD showed similar results.

FIGURE 6 Effects of TSG-6 on Inflammatory Phenotype and Marker Expression in Peritoneal Exudate Macrophages From ApoE$^{-/-}$ Mice

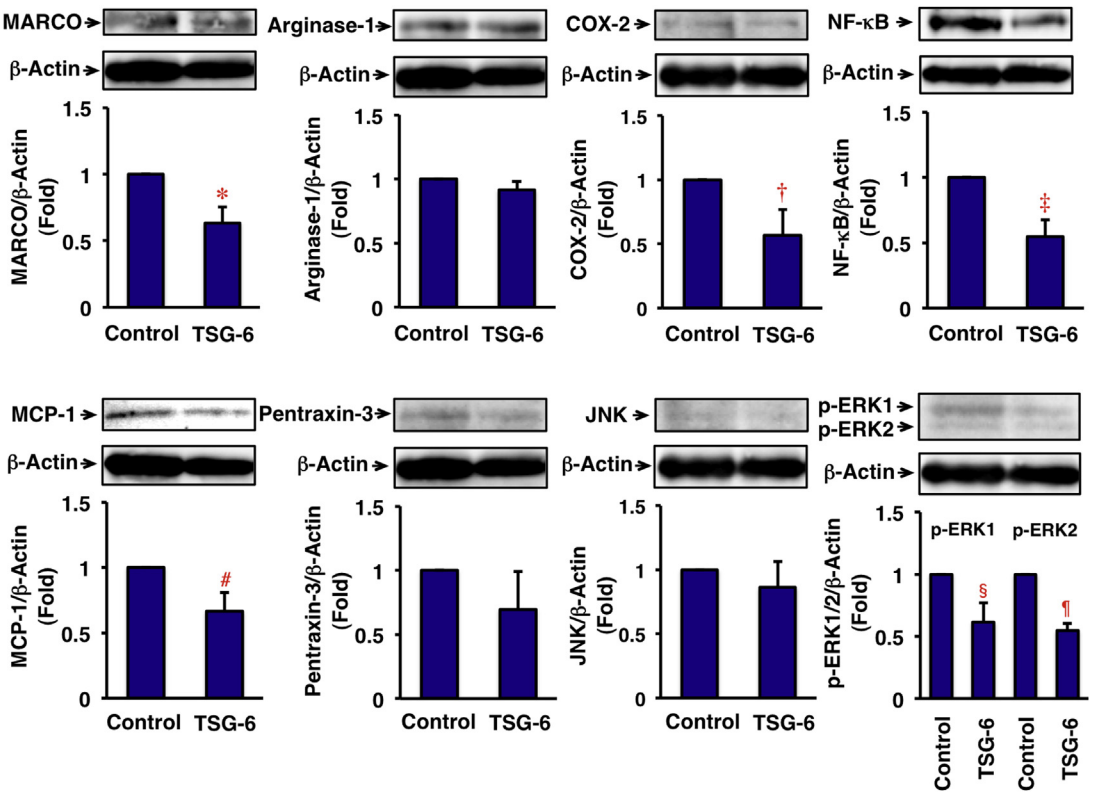

Peritoneal cells obtained from ApoE$^{-/-}$ mice were suspended in conditioned medium and seeded onto 6-cm dishes (4 × 10^6 cells per 2 ml/dish). After incubation for 1 h at 37°C in 5% CO_2 to allow adhesion, the medium was discarded to remove nonadherent cells. Immediately, adherent macrophages were harvested after washing the dishes with phosphate-buffered saline twice for immunoblotting analyses of MARCO (M1 marker), arginase-1 (M2 marker), MCP-1, pentratin-3, COX-2, NF-κB, JNK, and phosphorylated ERK1/2. β-actin served as a loading control. n = 3 to 5; *p = 0.018; †p = 0.031; ‡p = 0.012; #p = 0.041; §p = 0.038; ¶p < 0.0001 vs. control. All values are presented as mean ± SEM. Abbreviations as in Figures 3 and 5.

FIGURE 7 **Expression of TSG-6 in Human Coronary Arteries From Patients Without and With CAD**

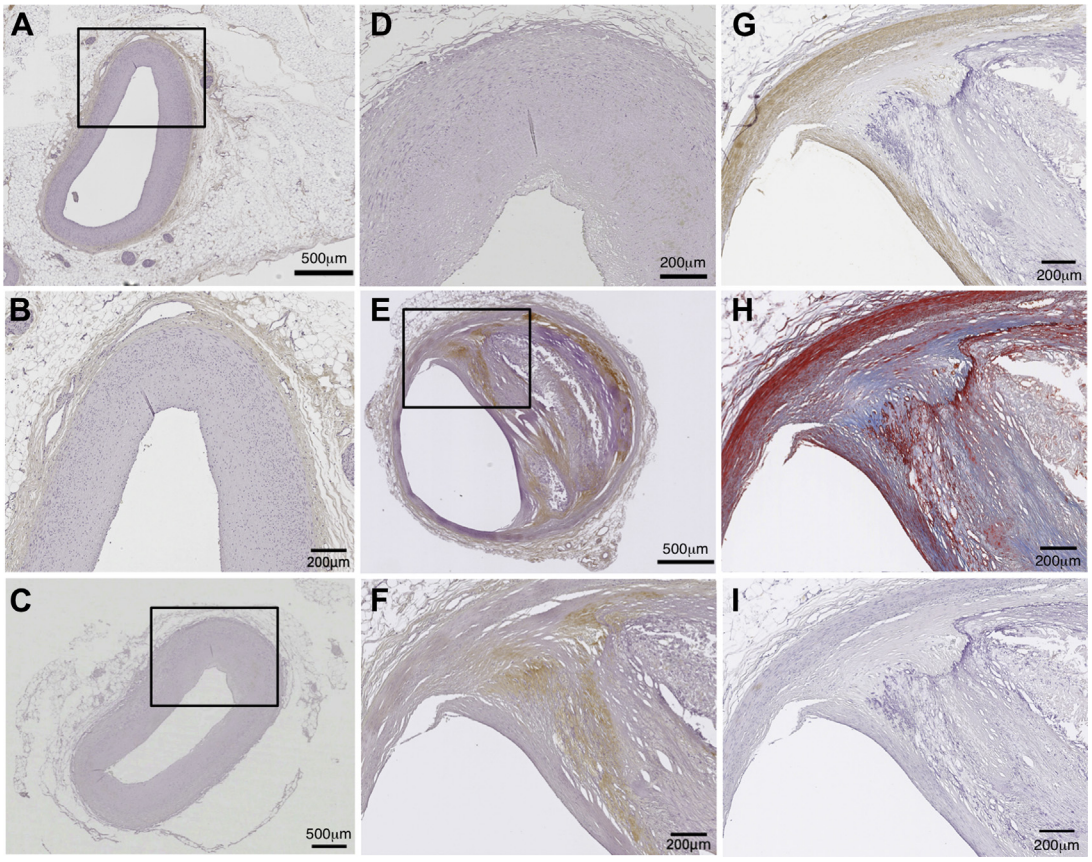

Representative normal coronary arteries **(A and B)** from a patient with dilated cardiomyopathy (male, age 34 years) and nonstenotic coronary arteries **(C and D)** from a patient with previous myocardial infarction (male, age 78 years), and representative stenotic coronary arteries **(E to I)** from a patient with previous myocardial infarction (male, age 62 years) were stained with anti-TSG-6 antibody **(A to F)**; anti-α-SMA antibody, a VSMC marker **(G)**; Masson's Trichrome, a collagen fiber marker **(H)**; and anti-CD68 antibody, a macrophage marker **(I)**. These patients died of heart failure or stroke. All coronary arteries were not the culprit artery of acute coronary events. CAD = coronary artery disease; other abbreviations as in Figure 5.

Next, plasma TSG-6 levels were compared between 47 patients without CAD and 135 patients with CAD. As listed in Table 3, age; prevalence of smoking, diabetes, and hypertension; and use of antidiabetic drugs were significantly greater and HDL cholesterol levels were significantly lower in patients with CAD than in subjects without CAD. The prevalence of several kinds of antihypertensive and antidyslipidemia drugs, and LDL cholesterol levels did not differ significantly between the 2 groups. As shown in Figure 8, plasma TSG-6 levels were significantly higher in patients with CAD than in subjects without CAD. Because a previous report showed increased TSG-6 levels in the airway secretions of smokers (28), we evaluated the relationship between plasma TSG-6 levels and smoking in patients without and with CAD. Plasma TSG-6 levels did not differ significantly between smokers and nonsmokers both in the non-CAD group (6.72 ± 1.24 vs. 7.89 ± 1.21; $p = 0.693$) and the CAD group (13.00 ± 0.93 vs. 10.90 ± 1.24; $p = 0.202$). In all subjects ($n = 182$), multiple linear regression analysis revealed that plasma TSG-6 levels were not significantly associated with age, and the prevalence of male, smoking, diabetes, and hypertension (all $p > 0.05$). Pearson's regression analysis confirmed no significant correlations of plasma TSG-6 levels with age ($r = 0.142$; $p = 0.056$; $n = 182$) or high-sensitivity CRP ($r = 0.033$; $p = 0.682$; $n = 161$). These findings suggest that TSG-6 in plasma may be a candidate for an independent biomarker of CAD.

TABLE 3 Patient Characteristics

	Non-CAD Subjects (n = 47)	CAD Patients (n = 135)	p Value
Male	68.1	75.6	0.317
Age, yrs	47.3 ± 2.5	70.8 ± 1.1	**<0.0001**
Smoking	14.9	69.6	**<0.0001**
Diabetes	8.5	31.1	**0.002**
Hypertension	53.2	72.6	**0.014**
Dyslipidemia	17.4	25.4	0.269
Antidiabetic drugs	2.1	17.2	**0.009**
ARBs	36.2	33.6	0.748
ACE inhibitors	0.0	4.5	0.140
Calcium-channel blockers	23.9	32.1	0.296
Beta-blockers	6.4	9.0	0.582
Statins	14.9	19.4	0.491
Fibrates	2.1	1.5	0.774
Eicosapentaenoic acids	4.3	4.5	0.942
LDL cholesterol, mg/dl	122.6 ± 5.06*	115.6 ± 3.09	0.291
HDL cholesterol, mg/dl	57.70 ± 1.97*	44.50 ± 0.95	**<0.0001**

Values are % or mean ± SEM. The p values in **bold** are statistically significant. *n = 34.
ACE = angiotensin-converting enzyme; ARB = angiotensin receptor blocker; HDL = high-density lipoprotein; LDL = low-density lipoprotein.

FIGURE 8 Plasma TSG-6 Levels in Patients Without and With CAD

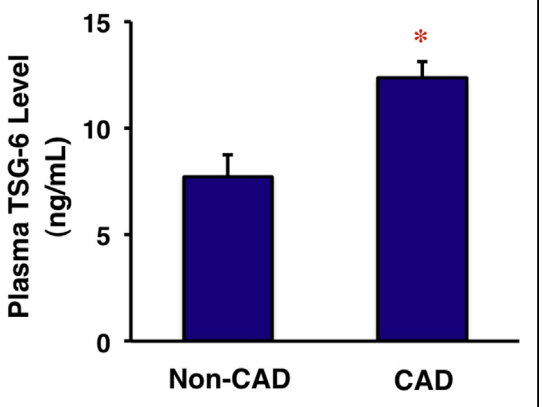

Plasma TSG-6 levels were measured by enzyme-linked immunosorbent assay in 47 subjects without CAD and 135 patients with acute coronary syndrome. *p < 0.005 vs. non-CAD. All values are presented as mean ± SEM. CAD = coronary artery disease; TSG-6 = tumor necrosis factor–stimulated gene-6.

DISCUSSION

This is the first demonstration that TSG-6 indeed suppresses the inflammatory response and cell proliferation in ECs, inflammatory phenotype and foam cell formation in HMDMs, and migration and proliferation of VSMCs in vitro. This study also showed that TSG-6 retards the development of aortic atherosclerotic lesions with decreased intraplaque contents of monocytes/macrophages and VSMCs in ApoE$^{-/-}$ mice in vivo. However, atherosclerotic plaque size in the aortic sinus was not completely suppressed by TSG-6. In our findings, TSG-6 increased collagen-1 and -3 expression in vitro and collagen fibers in atherosclerotic plaques in vivo, and TSG-6 was expressed at high levels in the fibrous cap within human coronary atherosclerotic plaques, which suggests that TSG-6 contributes to the stability of atherosclerotic plaques. Plasma TSG-6 levels are speculated to increase in patients with CAD, because chronic vascular inflammation stimulates TSG-6 production to counteract atherogenesis. Further analyses are required to clarify the relationship of decreased TSG-6 expression levels in the coronary plaque tissue and/or the circulating blood with plaque destabilization and rupture.

TSG-6 expression in macrophages, VSMCs, and fibroblasts was enhanced by LPS, FGF, and transforming growth factor-β (1). TSG-6 was also detected in the serum of patients with systemic lupus erythematosus and bacterial sepsis and of volunteers injected with bacterial LPS (29). Reportedly, TSG-6 contributes to stabilize murine eye lesions by its anti-inflammatory properties (30,31). Moreover, TSG-6 amplifies hyaluronan synthesis in murine airway SMCs (32). A previous study showed that TSG-6 exerts an anti-inflammatory function by counteracting the transcription of MMP-1 and -3 and the activation of MMP-1 in human fibroblasts (33). In the present study, up-regulation of collagens and MMPs by TSG-6 in VSMCs may be associated with vascular tissue injury, repair, and regeneration with inflammation (34). TSG-6 was shown to exert anti-inflammatory effects in several animal models. Administration of TSG-6 improved arthritis and diminished inflammation in several murine models (2,35). Our study showed that chronic TSG-6 infusion into ApoE$^{-/-}$ mice suppressed pentraxin-3 expression in aortic tissues and exudate peritoneal macrophages but not in plasma. In transgenic mice, knockout of the gene aggravated inflammatory responses (36), and overexpression of the gene decreased inflammatory responses (37). Further studies are needed to elucidate whether knockout of TSG-6 in ApoE$^{-/-}$ mice may accelerate the progression of atherosclerotic lesions.

The present results concerning the effect of TSG-6 on VSMC proliferation are inconsistent with a previous report. Ye et al. (12) showed that both rabbit aortic VSMCs and rat pulmonary VSMCs with overexpressing TSG-6 exhibited an increase in cell number in the serum-free culture system (12). In our

WST-8 assay, TSG-6 significantly suppressed HASMC proliferation in a concentration-dependent manner in a standard medium containing 5% FBS. The difference may be attributed to differences in species, methods of adding TSG-6 into cells, and presence or absence of sera. Our examination may be performed in human cells under more physiological conditions. However, TSG-6 did not significantly suppress HASMC proliferation induced by platelet-derived growth factor-BB in our preliminary examination (data not shown).

The specific receptors for TSG-6 have not yet been identified. It is especially important to elucidate the putative receptor, which provides an investigation of its agonist as a new drug target to treat atherosclerosis. The signal transduction pathways for TSG-6 have also been rarely reported. The present study suggests that TSG-6 suppresses the migration and proliferation of VSMCs via the down-regulation of c-Src, JNK, and NF-κB but may not induce apoptosis via both the up-regulation of Bcl-2, an antiapoptotic molecule, and the down-regulation of p38, a proapoptotic molecule (Supplemental Figure 2A). As exhibited in Supplemental Figure 3, the down-regulation of ERK1/2 may participate in the signals of which TSG-6 causes an M1 to M2 phenotype transition during the differentiation of human monocytes into macrophages (38). In mouse exudate macrophages, TSG-6 suppressed M1 phenotype and MCP-1 and COX-2 expression associated with the down-regulation of ERK1/2 and NF-κB.

We discuss the integrity of TSG-6 concentrations in our in vitro and in vivo experiments. First, the concentrations of TSG-6 required to modulate several responses of HMDMs, human ECs, and HASMCs were considerably high: 10- to 60-fold higher than plasma TSG-6 levels in humans (~5 ng/ml). In the vascular wall, large amounts of TSG-6 are mainly generated by vascular cells other than fibroblasts in an autocrine/paracrine manner. Animal and clinical studies showed that local levels of other vasoactive agents such as serotonin and AngII were increased by 10- to 100-fold with coronary events in obstructive arteries and cardiac interstitial fluid (39,40), which is comparable with the present study. Second, the TSG-6 level in human serum from a healthy volunteer was 7.4 ng/ml in the present study. Therefore, the 10% concentration added to the culture medium for human monocyte-macrophages (0.74 ng/ml) was negligible compared with the concentrations of human recombinant TSG-6 that were added. Third, the adequate concentrations of TSG-6 differed in inducing foam cell formation and related protein expression in HMDMs. This is mostly dependent on the difference in the presence or absence of oxLDL and their concerned signal transductions. TSG-6 at greater than adequate concentrations might lead to the down-regulation of the receptor and intracellular signals. Last, plasma TSG-6 levels in ApoE$^{-/-}$ mice infused with TSG-6 became significantly higher (~1.6 fold) than those of ApoE$^{-/-}$ mice infused with saline, which were not as high as expected. The peptide might be somewhat metabolized in circulating blood.

In the present study, other than the atheroprotective effects of TSG-6 in vitro, an important unexpected effect was observed in vivo. Chronic TSG-6 infusion in ApoE$^{-/-}$ mice significantly decreased plasma total cholesterol levels with a slight increase in HDL cholesterol levels. We speculate that TSG-6 may decrease intestinal cholesterol absorption, hepatic synthesis, and the assembly of very-low-density lipoprotein. In addition, it may increase hepatic LDL receptor expression, leading to a decrease in total cholesterol levels. Taken together, these findings may strengthen the clinical utility of TSG-6 in the prevention and treatment of atherosclerosis.

CONCLUSIONS

The present results indicate that TSG-6 retards the development of atherosclerotic lesions by decreasing plasma total cholesterol levels, inflammatory responses of ECs and HMDMs, macrophage foam cell formation, and the migration and proliferation of VSMCs. In addition, TSG-6 counteracts atherogenesis and contributes to plaque stability by promoting the production of collagen in the fibrous cap. Thus, TSG-6 replacement therapy, with either the peptide itself and/or its analogues, is expected to emerge as a new line of therapy against atherosclerosis and its related CAD. The results presented here also provide insights into the potential use of TSG-6 as a biomarker for CAD. These findings may strengthen the clinical utility of TSG-6 in the diagnosis and treatment of CAD.

ACKNOWLEDGMENTS The authors thank Ms. Kyoko Nohtomi, Ms. Yuuki Sato, Ms. Nana Ozawa, and Dr. Fumiko Itoh for technical assistance and helpful comments, respectively.

REPRINT REQUESTS AND CORRESPONDENCE: Prof. Takuya Watanabe, Laboratory of Cardiovascular Medicine, Tokyo University of Pharmacy and Life Sciences, 1432-1 Horinouchi, Hachioji-City, Tokyo 192-0392, Japan. E-mail: watanabe@toyaku.ac.jp.

PERSPECTIVES

COMPETENCY IN MEDICAL KNOWLEDGE: TSG-6 is regarded as an anti-inflammatory protein. Our cellular, animal, and clinical experiments demonstrate the protective effects of TSG-6 against vascular inflammation and atherosclerosis. TSG-6 also contributes to the stability of atherosclerotic plaques. Thus, TSG-6 may open a new therapeutic window for combating atherosclerosis and related CAD. In addition, our study provides insights into the potential use of TSG-6 as a biomarker for CAD.

TRANSLATIONAL OUTLOOK: The present study is the first to show that TSG-6 could be a candidate biomarker and therapeutic target for atherosclerotic cardiovascular diseases. Prospective studies concerning the clinical utility of TSG-6 in the diagnosis and treatment of CAD and outcomes over time may be warranted.

REFERENCES

1. Milner CM, Day AJ. TSG-6: a multifunctional protein associated with inflammation. J Cell Sci 2003;116:1863–73.

2. Bardos T, Kamath RV, Mikecz K, Glant TT. Anti-inflammatory and chondroprotective effect of TGF-6 (tumor necrosis factor-α stimulated gene-6) in murine models of experimental arthritis. Am J Pathol 2001;159:1711–21.

3. Lee RH, Pulin AA, Seo MJ, et al. Intravenous hMSCs improve myocardial infarction in mice because cells embolized in lung are activated to secrete the anti-inflammatory protein TSG-6. Cell Stem Cell 2009;5:54–63.

4. Lin QM, Zhao S, Zhou LL, Fang XS, Fu Y, Huang ZT. Mesenchymal stem cells transplantation suppresses inflammatory responses in global cerebral ischemia: contribution of TNF-α-induced protein 6. Acta Pharmacol Sin 2013;34:784–92.

5. Wisniewski HG, Maier R, Lotz M, et al. TSG-6: a TNF-, IL-1-, and LPS-inducible secreted glycoprotein associated with arthritis. J Immunol 1993;151:6593–601.

6. Fujimoto T, Savani RC, Watari M, Day AJ, Strauss JF 3rd. Induction of the hyaluronic acid-binding protein, tumor necrosis factor-stimulated gene-6, in cervical smooth muscle cells by tumor necrosis factor-α and prostaglandin E_2. Am J Pathol 2002;160:1495–502.

7. Lee TH, Wisniewski HG, Vilcek J. A novel secretory tumor necrosis factor-inducible protein (TSG-6) is a member of the family of hyaluronate binding proteins, closely related to the adhesion receptor CD44. J Cell Biol 1992;116:545–57.

8. Cao TV, La M, Getting SJ, Day AJ, Perretti M. Inhibitory effects of TSG-6 link module on leukocyte-endothelial cell interactions *in vitro* and *in vivo*. Microcirculation 2004;11:615–24.

9. Dyer DP, Thomson JM, Hermant A, et al. TSG-6 inhibits neutrophil migration via direct interaction with the chemokine CXCL8. J Immunol 2014;192:2177–85.

10. Mindrescu C, Le J, Wisniewski HG, Vilcek J. Up-regulation of cyclooxygenase-2 expression by TSG-6 protein in macrophage cell line. Biochem Biophys Res Commun 2005;330:737–45.

11. Choi H, Lee RH, Bazhanov N, Oh JY, Prockop DJ. Anti-inflammatory protein TSG-6 secreted by activated MSCs attenuates zymosan-induced mouse peritonitis by decreasing TLR2/NF-κB signaling in resident macrophages. Blood 2011;118:330–8.

12. Ye L, Mora R, Akhayani N, Haudenschild CC, Liau G. Growth factor and cytokine-regulated hyaluronan-binding protein TSG-6 is localized to the injury-induced rat neointima and confers enhanced growth in vascular smooth muscle cells. Circ Res 1997;81:289–96.

13. Wang SS, Hu SW, Zhang QH, Xia AX, Jiang ZX, Chen XM. Mesenchymal stem cells stabilize atherosclerotic vulnerable plaque by anti-inflammatory properties. PLOS ONE 2015;10:e0136026.

14. Ross R, Agius L. The process of atherogenesis-cellular and molecular interaction: from experimental animal models to humans. Diabetologia 1992;35 Suppl 2:S34–40.

15. Tabas I, Bornfeldt KE. Macrophage phenotype and function in different stages of atherosclerosis. Circ Res 2016;118:653–67.

16. Tiwari RL, Singh V, Barthwal MK. Macrophages: an elusive yet emerging therapeutic target of atherosclerosis. Med Res Rev 2008;28:483–544.

17. Watanabe T, Suguro T, Kanome T, et al. Human urotensin II accelerates foam cell formation in human monocyte-derived macrophages. Hypertension 2005;46:738–44.

18. Obikane H, Abiko Y, Ueno H, Kusumi Y, Esumi M, Mitsumata M. Effect of endothelial cell proliferation on atherogenesis: a role of $p21^{Sdi/Cip/Waf1}$ in monocyte adhesion to endothelial cells. Atherosclerosis 2010;212:116–22.

19. Watanabe K, Watanabe R, Konii H, et al. Counteractive effects of omentin-1 against atherogenesis. Cardiovasc Res 2016;110:118–28.

20. Watanabe T, Nishio K, Kanome T, et al. Impact of salusin-α and -β on human macrophage foam cell formation and coronary atherosclerosis. Circulation 2008;117:638–48.

21. Xu G, Watanabe T, Iso Y, et al. Preventive effects of heregulin-β1 on macrophage foam cell formation and atherosclerosis. Circ Res 2009;105:500–10.

22. Konii H, Sato K, Kikuchi S, et al. Stimulatory effects of cardiotrophin 1 on atherosclerosis. Hypertension 2013;62:942–50.

23. Hasegawa A, Sato K, Shirai R, et al. Vasoprotective effects of urocortin 1 against atherosclerosis in vitro and in vivo. PLOS ONE 2014;9:e110866.

24. Yamamoto K, Tajima Y, Hasegawa A, et al. Contrasting effects of stanniocalcin-related polypeptides on macrophage foam cell formation and vascular smooth muscle cell migration. Peptides 2016;82:120–7.

25. Naito C, Hashimoto M, Watanabe K, et al. Facilitatory effects of fetuin-A on atherosclerosis. Atherosclerosis 2016;246:344–51.

26. Watanabe J, Shetty AK, Hattiangady B, et al. Administration of TSG-6 improves memory after traumatic brain injury in mice. Neurobiol Dis 2013;59C:86–99.

27. Nagashima M, Watanabe T, Terasaki M, et al. Native incretins prevent the development of atherosclerotic lesions in apolipoprotein E knockout mice. Diabetologia 2011;54:2649–59.

28. Forteza R, Casalino-Matsuda SM, Monzon ME, et al. TSG-6 potentiates the antitissue kallikrein activity of inter-α-inhibitor through bikunin release. Am J Respir Cell Mol Biol 2007;36:20–31.

29. Lee TH, Wisniewski HG, Klampfer L, Oppenheim JD, Vilcek J. TSG-6: a novel secretory protein inducible by tumor necrosis factor or interleukin-1 in fibroblasts and mononuclear cells. In: Fiers W, Buurman WA, editors. Tumor Necrosis Factor: Molecular and Cellular Biology and Clinical Relevance. Basel: Karger, 1993:90–5.

30. Tuo J, Cao X, Shen D, et al. Anti-inflammatory recombinant TSG-6 stabilizes the progression of

focal retinal degeneration in a murine model. J Neuroinflammation 2012;9:59.

31. Oh JY, Roddy GW, Choi H, et al. Anti-inflammatory protein TSG-6 reduces inflammatory damage to the cornea following chemical and mechanical injury. Proc Natl Acad Sci U S A 2010; 107:16875–80.

32. Lauer ME, Cheng G, Swaidani S, Aronica MA, Weigel PH, Hascall VC. Tumor necrosis factor-stimulated gene-6 (TSG-6) amplifies hyaluronan synthesis by airway smooth muscle cells. J Biol Chem 2013;288:423–31.

33. Guo P, Zhang SZ, He H, Zhu YT, Tseng SC. TSG-6 controls transcription and activation of matrix metalloproteinase 1 in conjunctivochalasis. Invest Ophthalmol Vis Sci 2012;53:1372–80.

34. Mahoney DJ, Mulloy B, Forster MJ, et al. Characterization of the interaction between tumor necrosis factor-stimulated gene-6 and heparin: implications for the inhibition of plasmin in extracellular matrix microenvironments. J Biol Chem 2005;280:27044–55.

35. Mindrescu C, Thorbecke GJ, Klein MJ, Vilcek J, Wisniewski HG. Amelioration of collagen-induced arthritis in DBA/1J mice by recombinant TSG-6, a tumor necrosis factor/interleukin-1-inducible protein. Arthritis Rheum 2000;43:2668–77.

36. Szántó S, Bárdos T, Gál I, Glant TT, Mikecz K. Enhanced neutrophil extravasation and rapid progression of proteoglycan-induced arthritis in TSG-6-knockout mice. Arthritis Rheum 2004;50:3012–22.

37. Mindrescu C, Dias AA, Olszewski RJ, Klein MJ, Reis LF, Wisniewski HG. Reduced susceptibility to collagen-induced arthritis in DBA/1J mice expressing the TSG-6 transgene. Arthritis Rheum 2002;46:2453–64.

38. De Paoli F, Staels B, Chinetti-Gbaguidi G. Macrophage phenotypes and their modulation in atherosclerosis. Circ J 2014;78:1775–81.

39. Leosco D, Fineschi M, Pierli C, et al. Intracoronary serotonin release after high-pressure coronary stenting. Am J Cardiol 1999;84:1317–22.

40. Schuijt MP, van Kats JP, de Zeeuw S, et al. Cardiac interstitial fluid levels of angiotensin I and II in the pig. J Hypertens 1999;17:1885–91.

KEY WORDS **atherosclerosis, coronary artery disease, endothelial cell, macrophage, TSG-6, vascular smooth muscle cell**

APPENDIX **For supplemental figures, please see the online version of this article.**